Breakdown of the Mott insulator:
Exact solution of an asymmetric Hubbard model

Takahiro Fukui*

Institute of Advanced Energy, Kyoto University, Uji, Kyoto 611, Japan

Norio Kawakami

Department of Applied Physics, Osaka University, Suita, Osaka 565, Japan
(December 1, 1997)

The breakdown of the Mott insulator is studied when the dissipative tunneling into the environment is introduced to the system. By exactly solving the one-dimensional asymmetric Hubbard model, we show how such a breakdown of the Mott insulator occurs. As the effect of the tunneling is increased, the Hubbard gap is monotonically decreased and finally disappears, resulting in the insulator-metal transition. We discuss the origin of this quantum phase transition in comparison with other non-Hermitian systems recently studied.

PACS: 71.27.+a, 71.30.+h, 05.30.-d

I. INTRODUCTION

Strongly correlated electron systems in low dimensions have attracted renewed interest since the discovery of the high-T_c superconductivity [1,2]. In particular, systematic study of electron systems in the Mott insulating phase is believed to provide an important key step to understand such unconventional phenomena [3]. To clarify correlation effects on the Mott insulator [4–6], it is efficient to probe the response of the system to external fields. For semiconductors with weak correlations, the charge gap due to the one-body band structure is collapsed by strong external electric fields, which is well-known as the Zener breakdown [7]. For the Mott insulator, however, it is not straightforward to study such a problem theoretically, because it is essentially a non-equilibrium many-body problem. To observe the breakdown of the Mott insulator may indeed provide new paradigm for strongly correlated electron systems in non-equilibrium conditions. Although there have not been many works in this context so far, such attempts have been recently started experimentally [8].

In this paper, we address the problem how such breakdown phenomena occur for the Mott insulators in non-equilibrium conditions. Since it seems still difficult to deal with the Zener breakdown directly, we here propose a related simple model, and study its properties exactly. Namely, as a typical example of the Mott insulator, we investigate the one-dimensional (1D) Hubbard model with *the dissipative tunneling into the environment*, which has a non-Hermitian character. By using the exact solution of the model, we show that *there exits a critical strength of the tunneling, at which the Hubbard gap is closed and the insulator-metal transition occurs*. We determine the phase diagram by calculating the critical line exactly.

One of the characteristic aspects in our model is that the effect of the asymmetric tunneling gives rise to imaginary gauge potential, which may be regarded as a generalization of a conventional (real) gauge potential induced by twisted boundary conditions [9–13]. In this connection, we wish to note that such unconventional systems with imaginary gauge potential have attracted much current interest for 1D random systems [14–20] and spin systems [21–29]. In particular, Hatano and Nelson [14] have recently shown that the delocalization transition for the pinned flux state of superconductors in cylinder geometry can be described by a 1D tight-binding model with asymmetric hoppings. They have demonstrated the importance of the imaginary gauge potential due to the non-Hermitian hopping term, which can indeed delocalize the "insulating" state caused by the randomness. This type of delocalization phenomenon indeed happens even for the Mott insulator, as discussed in the next section, and both phenomena have a close relationship to each other, except that the insulating phase in the present case is formed by the electron correlation, not by the randomness. This mechanism is also applied to the collapse of the Ising-type spin gap for the asymmetric XXZ model, which has been found in ref. [22,25].

This paper is organized as follows. In Sec. II, we introduce the model Hamiltonian, and mention the relationship to 1D disordered systems with an imaginary vector potential and also to the asymmetric XXZ model. In sec. III, we solve the model by means of the Bethe ansatz method, and show how the insulator-metal transition occurs when the tunneling amplitude is increased. We discuss characteristic properties in the insulating phase and the metallic phase separately. In Sec. IV, we summarize our results.

II. MODEL HAMILTONIAN

Let us start with the ordinary 1D Hubbard model with the on-site repulsive Coulomb interaction U. When an external bias voltage is applied between the first site and

the last site, it induces non-equilibrium currents, which may be essential for the dissipation into the environment. In order to effectively formulate the tunneling of electron currents into the environment, we introduce asymmetric tunneling (or hopping) terms at two end points (1st and Lth sites), namely the asymmetry between $T_{L1}c_{L\sigma}^\dagger c_{1\sigma}$ and $T_{1L}c_{1\sigma}^\dagger c_{L\sigma}$ with real amplitudes $T_{1L} \neq T_{L1}$. For example, when $T_{L1} < T_{1L}$, we can effectively describe the situation where electrons may be supplied at the first site, and may dissipate at another boundary. It may be thus expected that this type of asymmetric tunneling at boundaries may describe some essential features, especially a "direction" for the system, caused by non-equilibrium currents.

In order for the tunneling rate into the environment to be a macroscopic quantity, T_{L1} (T_{1L}) should be extensive. To obtain physically sensible result, it is convenient to parameterize them as boundary conditions, $c_{L+1\sigma} = e^{-L\Psi}c_{1\sigma}$ and $c_{L+1\sigma}^\dagger = e^{L\Psi}c_{1\sigma}^\dagger$, where Ψ (order of unity) controls the strength of the asymmetric tunneling. In this case, we have $T_{L1} = -te^{-L\Psi}$ and $T_{1L} = -te^{L\Psi}$. This expression implies that the present boundary condition can be regarded as a twisted boundary condition with an *imaginary* twist angle. Recall that the ordinary twisted boundary condition is equivalent to introducing a magnetic flux threaded in the ring system [30,10]. Similarly, the imaginary twisted boundary condition in our model effectively induces the imaginary gauge potential in a ring system [14]. Namely, if we use a gauge transformation, the Hamiltonian is now cast into the form with periodic boundary conditions,

$$H = -t\sum_{j=1}^{L}\sum_{\sigma}\left(e^{-\Psi}c_{j\sigma}^\dagger c_{j+1\sigma} + e^{\Psi}c_{j+1\sigma}^\dagger c_{j\sigma}\right)$$
$$+U\sum_{j=1}^{L}n_{j\uparrow}n_{j\downarrow}, \tag{1}$$

where $U \geq 0$. It is clearly seen that each hopping term acquires imaginary gauge potential Ψ. The eigenvalues of the Hamiltonian always appear in complex conjugate pairs. Since $H^\dagger(\{\psi_j\}) = H(-\{\psi_j\})$, the right-eigenvector of $H(\{\psi_j\})$ is equivalent to left-eigenvector of $H(-\{\psi_j\})$ with the same energy.

It is to be noticed that the Hamiltonian is *non-Hermitian*, because we have eliminated the environment by introducing the asymmetric tunneling instead, which as a result causes dissipative effects. The non-Hermitian property may be natural since we are now concerned with non-equilibrium phenomena. In the gauge-transformed representation (1), the hopping term feels an imaginary gauge field Ψ at every site. Now the relationship to the 1D disordered tight-binding models with an imaginary vector potential [14–18] and the asymmetric XXZ model [21–29] is clear: The hopping term in Eq. (1) takes essentially the same form as found in such models.

The difference among them is the mechanism to realize the insulating phases when $\Psi = 0$: The Mott insulator is stabilized by the Hubbard interaction for the present model, whereas the Anderson insulator is realized by random potentials for disordered tight-binding models, and the spin-gapped state appears by the Ising-anisotropy for the asymmetric XXZ model. Therefore, the present insulator-metal transition may have essentially the same origin as for the Hatano-Nelson model [14] and also the asymmetric XXZ model [22,28].

In the next section, we show that the charge gap of the present system closes due to the asymmetric tunneling effects, and consequently the Mott insulator breaks down.

III. BETHE ANSATZ EQUATIONS

Let us now turn to the solution of the above Hamiltonian. The Bethe ansatz method still works even for such unconventional Hamiltonian, because asymmetric hoppings in the model are incorporated as twisted boundary conditions with *imaginary twist angle* [31,32], as mentioned above. In fact, the asymmetric XXZ model have been extensively investigated by the Bethe ansatz method [21–29]. It has been shown that the gap due to Ising-anisotropy closes when the imaginary twist is increased [22,28]. Now, applying the Bethe-ansatz technique to our model, we diagonalize the Hamiltonian (1) to obtain the Bethe-ansatz equations [10,33–35],

$$k_j L = 2\pi I_j + iL\Psi + \sum_{\beta=1}^{N_\downarrow}\theta(\sin k_j - \lambda_\beta),$$
$$\sum_{j=1}^{N}\theta(\sin k_j - \lambda_\alpha) = 2\pi J_\alpha - \sum_{\beta=1}^{N_\downarrow}\theta\left(\frac{\lambda_\alpha - \lambda_\beta}{2}\right), \tag{2}$$

where the two-body phase shift is $\theta(x) = -2\arctan(x/u)$ with $u = U/(4t)$. Here the quantum numbers are $I_j = N_\downarrow/2 \pmod 1$ and $J_\alpha = (N - N_\downarrow + 1)/2 \pmod 1$. The branch cut of θ is set along $(-i\infty, -ic)$ and $(+ic, +i\infty)$. The energy of the whole system is given by $E = -2t\sum_{j=1}^{N}\cos k_j$.

In what follows, we consider the half-filling case, where the Mott insulating phase realizes for any finite U when $\Psi = 0$. Hence, we set the number of electrons $N = L$ and the number of down-spins $N_\downarrow = L/2$. In Fig. 1, we show the distribution of the rapidities on the complex k and λ plain, which are calculated directly by Eq. (2) for a small system. At $\Psi = 0$, all rapidities are on the real axis, whereas they form nontrivial curves on the complex plane for a finite Ψ. Their distributions are always symmetric with respect to the imaginary axis, which ensures that *the ground state energy is real*. Though imaginary twisted boundary conditions are imposed on the charge sector, the spin distribution is also affected slightly.
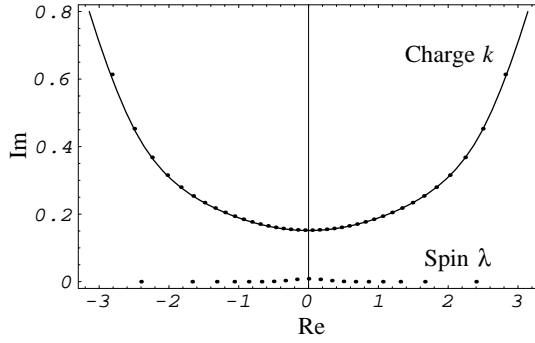
2

FIG. 1. Ground-state distribution of rapidities for the $L = 38$ system (half filling) with $u = 1$ and $b = 0.8$ ($\Psi = 0.242797$). The system with $u = 1$ has $b_{cr} = 0.881374$ ($\Psi_{cr} = 0.246349$). The solid curve is the distribution of charge rapidities in the bulk limit calculated numerically by Eq. (3). The horizontal and vertical axes are, respectively, real and imaginary part of k and λ.

A. Insulating phase

In order to study critical properties of the model, we should carefully observe the behavior of rapidities. To this end, let us define the counting functions, as usual, $z_c(k)$ and $z_s(\lambda)$ satisfying $z_c(k_j) = I_j/L$ and $z_s(\lambda_\alpha) = J_\alpha/L$, respectively. In the bulk limit, they are given by

$$z_c(k) = \frac{k}{2\pi} - \frac{i\Psi}{2\pi} - \frac{1}{2\pi}\int_{\mathcal{S}} d\lambda\theta(\sin k - \lambda)\sigma(\lambda), \qquad (3)$$

$$z_s(\lambda) = \frac{1}{2\pi}\int_{\mathcal{C}} dk\theta(\sin k - \lambda)\rho(k)$$
$$+ \frac{1}{2\pi}\int_{\mathcal{S}} d\lambda'\theta\left(\frac{\lambda - \lambda'}{2}\right)\sigma(\lambda'), \qquad (4)$$

where the distribution functions are $\rho(k) = z_c'(k)$ and $\sigma(\lambda) = z_s'(\lambda)$, satisfying

$$\rho(k) = \frac{1}{2\pi} - \frac{\cos k}{2\pi}\int_{\mathcal{S}} d\lambda\theta'(\sin k - \lambda)\sigma(\lambda), \qquad (5)$$

$$\sigma(\lambda) = -\frac{1}{2\pi}\int_{\mathcal{C}} dk\theta'(\sin k - \lambda)\rho(k)$$
$$+ \frac{1}{4\pi}\int_{\mathcal{S}} d\lambda'\theta'\left(\frac{\lambda - \lambda'}{2}\right)\sigma(\lambda'), \qquad (6)$$

and where $\mathcal{C}$ and $\mathcal{S}$ denote the curves on which the solutions of the rapidities lie.

Now, starting from the Mott insulating phase realized for small Ψ, we wish to deduce the critical point at which the Mott insulator breaks down. For this purpose we need to study the analytic properties of the ground state. First, we denote the end points of the curve $\mathcal{C}$ as $a + ib$ with $a = \pm\pi$ in the bulk limit, whereas those of $\mathcal{S}$ are $\pm\infty$. In the complex k plane, the poles of $\theta'(\sin k - \lambda)$ in Eq. (5) nearest to the real axis are $\pm i\,\mathrm{arcsinh}\,u$ (mod π). Therefore, if $b \leq b_{cr}$, where

$$b_{cr} \equiv \mathrm{arcsinh}\,u, \qquad (7)$$

$\mathcal{C}$ and $\mathcal{S}$ can be deformed, respectively, as $-\pi + ib \to -\pi \to \pi \to \pi + ib$ and $-\infty \to \infty$ with straight segments. Then the distribution functions are given by the analytic continuation of those with $\Psi = 0$, which means that *the system is still in the insulating phase*. For reference, we plot the curve $\mathcal{C}$ calculated by Eq. (3) in the bulk limit as a solid line in Fig. 1, from which one can observe that rapidities for a finite-size system sit exactly on $\mathcal{C}$ of the bulk limit except for the end ones which deviate slightly.

Since b characterizes the curve $\mathcal{C}$, there is one-to-one correspondence between Ψ and b. By using $z_c(k = \pm\pi + ib) = \pm 1/2$ in Eq. (3), which is valid by definition, we obtain the relation between Ψ and b,

$$\Psi(b) = b - i\int_{-\infty}^{\infty} d\lambda\theta(\lambda + i\sinh b)\sigma(\lambda). \qquad (8)$$

Eventually, we can determine the critical value of Ψ by the formula $\Psi_{cr} = \lim_{b \to b_{cr} - 0} \Psi(b)$ with Eq. (7), at which the analytic property of the ground state changes, namely, the breakdown of the Mott insulator occurs. In Fig. 2, we plot the critical values of Ψ_{cr} as a function of u. For small u, the Hubbard gap is exponentially small, and hence it is easily collapsed by small Ψ. For large u, we have the dependence of $\Psi_c \sim \mathrm{arcsinh}\,u$, so that we observe the crossover behavior around $u = 1$.
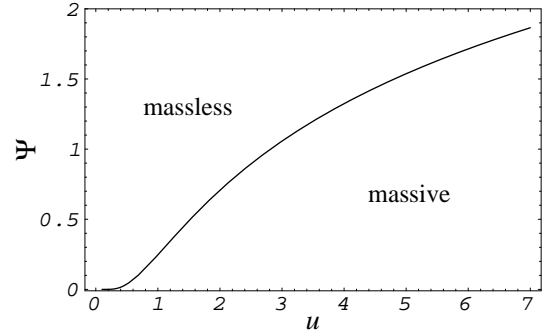

FIG. 2. Phase diagram for the insulator-metal transition. The solid line is the critical line $\Psi = \Psi_{cr}(u)$.

1. Hubbard Gap

Now that we have determined the critical Ψ_c in terms of singular properties in the ground state, let us directly evaluate the Hubbard gap to confirm it. At $\Psi = 0$, the charge excitation has the Hubbard gap for any finite U. We will show that the gap becomes smaller as Ψ is increased, and is finally collapsed at $\Psi = \Psi_{cr}$. The Hubbard gap is here defined [34] by $\Delta = U - 2\mu_-$, where the chemical potential μ_- is given by $\mu_- = E(N_\uparrow, N_\downarrow) - E(N_\uparrow - 1, N_\downarrow)$. To obtain μ_- in terms of a one-hole excitation energy, let us make a hole

state at I_h in consecutive quantum numbers I_j. Then we readily find that the energy change $\epsilon(k_h) = E - E_{\text{g.s.}}$ is given by the analytic continuation of that with $\Psi = 0$,

$$\epsilon(k_h) = 2t\left[\cos k_h + \int_{-\infty}^{\infty} d\omega \frac{e^{i\omega \sin k_h} J_1(\omega)}{\omega(1 + e^{2u|\omega|})}\right], \qquad (9)$$

where k_h corresponds to the rapidity of the hole I_h. The lowest charge excitation at $k_h = \pm\pi + ib$ determines the Hubbard gap. Therefore, setting $\mu_- = -\epsilon(\pm\pi + ib)$, we reach the expression for the Hubbard gap for finite Ψ,

$$\Delta(b) = 4t\left[u - \cosh b + \int_{-\infty}^{\infty} d\omega \frac{e^{\omega \sinh b} J_1(\omega)}{\omega(1 + e^{2u|\omega|})}\right], \quad (10)$$

where $J_n(\omega)$ is the nth Bessel function. It is now checked that the Hubbard gap is a monotonically decreasing function of Ψ, which confirms that the dissipative tunnelings into the environment indeed deduce the Hubbard gap. To evaluate the gap at $\Psi = \Psi_{\text{cr}}$, it is convenient to rewrite the expression,

$$\Delta(b)/4t = u - \cosh b - \sum_{n=1}^{\infty} (-)^n\left[\sqrt{1 + (2un - \sinh b)^2}\right.$$
$$\left. + \sqrt{1 + (2un + \sinh b)^2} - 4un\right]. \qquad (11)$$

It is readily seen that $\Delta(b_{\text{cr}}) = 0$, by setting $\sinh b_{\text{cr}} = u$. Namely, at $\Psi = \Psi_{\text{cr}}$ which has been determined by the analytic property of the ground state, the Hubbard gap indeed closes. Note that the expressions for the gap in this subsection is valid only for $\Psi \le \Psi_{\text{cr}}$, i.e., $b \le b_{\text{cr}}$. Therefore, we can confirm that *on the critical line in the phase diagram Fig. 2, the breakdown of the Mott insulator occurs due to the effect of dissipative tunnelings.*

2. Charge excitations

Next let us discuss how densely the charge excitation is distributed above the Hubbard gap. It is usually discussed by introducing the distribution function for charge excitations, $D(\varepsilon) = \partial z_c / \partial\varepsilon$, where $\varepsilon(k_h) \equiv 4t[c + \epsilon(k_h)/2t]$ with Eq. (9), taking the gap into account. For the present model, however, it may be more suitable to define it as

$$D(\varepsilon) \equiv \frac{\text{Re}\rho}{|\text{Re}\varepsilon'|}, \qquad (12)$$

since the energy of the elementary hole excitation is complex in general. Here, we evaluate ρ and ε along the curve $\mathcal{C}$ in the bulk limit calculated by using Eq. (3), e.g., the solid-curve in Fig. 1. We shall refer to $D(\epsilon)$ as the density of states (DOS) for simplicity.

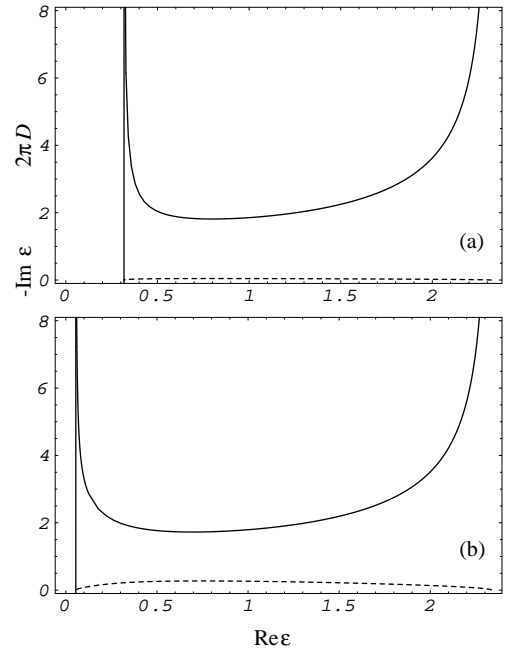In Fig. 3, we show DOS (12) for $u = 1$ case. One can see that at the band edge, DOS diverges as is the case

FIG. 3. Density of states (solid-line) for charge excitations and imaginary part of the excitation energy (dashed-line) for $u = 1$ system with b=0.1 (a) and b=0.8 (b). The corresponding Ψ is 0.0399396 for (a) and 0.242797 for (b), respectively. We here set $4t = 1$. The straight line is a guide for gaps.

for the conventional 1D Hubbard model. For reference, we also plot the imaginary part of the excitation energy ε. Here, since $\text{Im}\varepsilon(-k_h) = -\text{Im}\varepsilon(k_h)$, we plot $-\text{Im}\varepsilon(k_h)$ for $k_h \ge 0$. For a small Ψ [Fig. 3 (a)], eigenvalues are almost real, and behavior of the DOS is quite similar to $\Psi = 0$ system, as should be expected. As Ψ increases the charge gap certainly decreases. For a large Ψ near Ψ_{cr} [Fig. 3 (b)], DOS still diverges.

Now we observe the properties around the band edge in a bit detail. To this end, we need to calculate ρ and ε' at $k = \pi + ib_{\text{cr}}$. In a similar way to Eq. (11), we have

$$2\pi\rho(\pi + ib) = 1 - \cosh b \sum_{n=1}^{\infty} (-)^{n+1}$$

$$\times\left[\frac{1}{\sqrt{(2un - \sinh b)^2 + 1}} + \frac{1}{\sqrt{(2un + \sinh b)^2 + 1}}\right]. \quad (13)$$

Therefore,

$$\rho(\pi + ib_{\text{cr}}) = 0,$$
$$\rho'(\pi + ib_{\text{cr}}) = i(u^2 + 1)F(u)/\pi,$$
$$\rho''(\pi + ib_{\text{cr}}) = 3c\sqrt{u^2 + 1}F(u)/\pi, \qquad (14)$$

where

$$F(u) = \sum_{n=0}^{\infty} (-)^n \frac{(2n + 1)u}{\sqrt{(2n + 1)^2 u^2 + 1}^3}. \qquad (15)$$

Here we calculate ρ' and ρ'' for later convenience. We now find that near the critical point ρ is real and ap-

proaches to 0 as $\rho(\pi + ib) \sim -i\rho'(\pi + ib_{\mathrm{cr}})(b_{\mathrm{cr}} - b)$. Therefore, at first sight, the DOS defined by (12) does not seem to diverge at the band edge. However, noting $\varepsilon(\pi + ib) = \Delta(b)$, we have

$$\varepsilon'(\pi + ib_{\mathrm{cr}})/4t = iu - i\sqrt{u^2 + 1} \int_{-\infty}^{\infty} d\omega \frac{e^{u\omega} J_1(\omega)}{1 + e^{2u|\omega|}}. \quad (16)$$

Namely, $\varepsilon'(\pi + ib_{\mathrm{cr}})$ is pure imaginary. Therefore, the DOS of the system near the critical point diverges at the band edge, as is seen in Fig. 3 (b) [so far as we use the definition (12)], although ρ approaches 0. Anyway, the excitation above the Hubbard gap is unconventional with complex energy, which reflects the fact that the present system possesses non-Hermitian tunneling to the environment. Thus, when the Mott insulator breaks down, the resulting metallic state would have a dissipative character with complex eigen energy.

B. Metallic phase

So far we have shown that the Mott insulator breaks down at $\Psi = \Psi_{\mathrm{cr}}$. Now the question is what kind of state is realized beyond the critical Ψ_c. We shall show that it is a dissipative metallic phase without charge excitation gap. Let us recall first that in the Mott insulating phase, the real part of rapidities completely fills up the lower Hubbard band in the region $[-\pi, \pi]$. In order for the system to enter the metallic phase, the "Fermi points" $\pm a$ for the real part of the rapidity should leave away from $\pm \pi$, when we increase $\Psi > \Psi_c$. Indeed, from the expression (13) we see that $\rho(\pi + ib)$ decreases if we increase b and eventually at $b = b_{\mathrm{cr}}$, $\rho(\pi + ib_{\mathrm{cr}}) = 0$. Hence we have $a < \pi$ when $b > b_{\mathrm{cr}}$. To explicitly determine the Fermi points a (and b as well), we deform the curves $\mathcal{C}$ and $\mathcal{S}$ as the straight segments $-a + ib \to a + ib$ and $-\infty + i\lambda_1 \to \infty + i\lambda_1$, respectively. Consistency between Eq. (6) and $\int_{\mathcal{S}} d\lambda\sigma(\lambda) = 1/2$ requires

$$\sinh b - u < \lambda_1 < \cos a \sinh b + u. \quad (17)$$

Similarly, from Eq. (5) and $\int_{\mathcal{C}} dk\rho(k) = 1$ [or from Eq. (3)], we have,

$$1 = \frac{a}{\pi} - \frac{1}{2\pi} \int_{-\infty + i\lambda_1}^{\infty + i\lambda_1} d\lambda\sigma(\lambda) \Big\{ \theta\left(\sin(a + ib) - \lambda\right)$$
$$- \theta\left(\sin(-a + ib) - \lambda\right) \Big\}. \quad (18)$$

By using Eq. (3), corresponding Ψ is given by

$$\Psi = i(\pi - a) + b + i \int_{-\infty + i\lambda_1}^{\infty + i\lambda_1} d\lambda\theta\left(\sin(a + ib) - \lambda\right)\sigma(\lambda). \quad (19)$$

These are the basic equations to determine the effective "Fermi points" $\pm a$.

Let us solve these equations explicitly for two limiting cases. First, consider the large Ψ region, namely the limiting case of strong dissipation. When $b \to \infty$, we have $a \to 0$ with $0 < a^2 e^b/2 < 2u$ from the relation (17), and hence $\sin(\pm a + ib) - \lambda - i\lambda_1 \sim \pm ae^b - \lambda + iu' \to \pm\infty + iu'$, where $-u < u' < u$ due to Eq. (17). Then $\theta\left(\sin(\pm a + ib) - \lambda - i\lambda_1\right) \to \mp[\pi + 2u/(a^2 e^b)]$. Finally, from Eqs. (18) and (19), we end up with

$$\frac{1}{2} a^2 e^b = \frac{u}{\pi}, \quad \Psi = b. \quad (20)$$

This equation states that for a large Ψ, a indeed approaches 0 in the form $a \propto e^{-\Psi/2}$. Therefore, we can say that a large enough Ψ effectively drives the system to the low-density limit of the ordinary Hubbard model except that the energy eigenvalues are now complex reflecting a dissipative metallic state.

Next consider the metallic phase just beyond the critical point. Setting $a = \pi - \delta a$ and $b = b_{\mathrm{cr}} + \delta b$, we have $2\sqrt{u^2 + 1}\delta b < u(\delta a)^2/2$ from Eq. (17). Hence we see $\delta b = O(\delta a^2)$. Similarly, setting $\rho(k + ib) = \rho_{\mathrm{cr}}(k + ib) + \delta\rho(k)$ and $\sigma(\lambda + i\lambda_1) = \sigma_{\mathrm{cr}}(\lambda + i\lambda_1) + \delta\sigma(\lambda)$, where ρ_{cr} and σ_{cr} are distribution functions on the critical point, we immediately find $\delta\sigma(\lambda) = O(\delta a^3)$ by expanding Eqs. (5) and (6) in power series of δa and δb. Then Eqs. (18) and (19) reduce to

$$\delta a = \int_{-\infty}^{\infty} d\lambda\sigma_{\mathrm{cr}}(\lambda) \left[\theta'\delta a + i\theta''\delta a\delta b + \frac{1}{6}\theta'''\delta a^3\right] + O(\delta a^4),$$
$$\delta\Psi = i\delta a + \delta b$$
$$+ i \int_{-\infty}^{\infty} d\lambda\sigma_{\mathrm{cr}}(\lambda) \left[-\theta'\delta a + \frac{1}{2}\theta''\delta a^2\right] + O(\delta a^3), \quad (21)$$

where $\delta\Psi = \Psi - \Psi_{\mathrm{cr}}$, and $\theta' = \partial\theta(\sin k - \lambda)/\partial k|_{k=\pi+i(b_{\mathrm{cr}}-0)}$. Contributions from $\delta\sigma$ are included in higher order terms. A little algebra leads us to the final relations

$$\delta b = \frac{\rho_{\mathrm{cr}}''(\pi + ib_{\mathrm{cr}})}{6[-i\rho_{\mathrm{cr}}'(\pi + ib_{\mathrm{cr}})]}\delta a^2 + O(\delta a^3),$$
$$\delta\Psi = \left\{1 + \frac{6\pi[i\rho_{\mathrm{cr}}'(\pi + ib_{\mathrm{cr}})]^2}{\rho_{\mathrm{cr}}''(\pi + ib_{\mathrm{cr}})}\right\}\delta b + O(\delta a^3), \quad (22)$$

where ρ' and ρ'' are given by Eq. (14).

The flow of the end points is schematically illustrated in Fig. 4 as a function of Ψ. We can now see how the Hubbard gap disappears at half-filling: The larger Ψ is, the longer the curve $\mathcal{C}$ becomes (see Fig. 1). As a result, the density of charge rapidities at the end points $(\pm\pi)$ decreases and vanishes at $\Psi = \Psi_{\mathrm{cr}}$ [see Eq. (14)]. If we further increase Ψ, the end points (Fermi points) are forced to be away from π, realizing the metallic state. It is to be noted again that this metallic phase has a dissipative character with complex eigenvalues, which shows sharp contrast to the ordinary metallic phase.
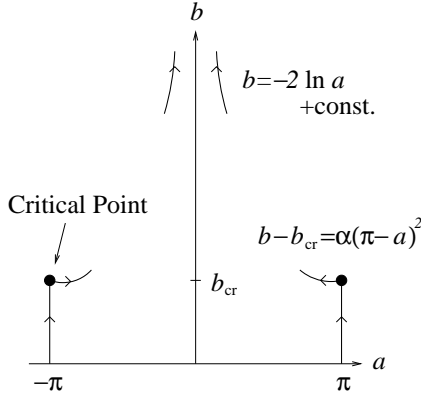
FIG. 4. Schematic illustration of the behavior of the end points $\pm a + ib$. They move toward the direction indicated by arrows if we increase Ψ.

IV. SUMMARY

In summary, we have proposed a non-Hermitian Hubbard model to study the insulator-metal transition, which may describe a many-body analogue of the Zener breakdown, driven by asymmetric tunneling into the environment. By solving the model exactly, we have shown that such a tunneling indeed causes the breakdown of the Mott insulator, and drives the system to a metallic state. We have studied the basic properties of the insulating phase and the metallic phase, and clarified the mechanism of the transition. In the sense that this transition is caused by the imaginary gauge potential induced by the asymmetric tunneling, it shares essential properties with other interesting non-Hermitian systems such as the model of Hatano and Nelson for the delocalization of pinned flux state in superconductors and also the collapse of the Ising-type spin gap for the asymmetric XXZ spin chain. Although the experimental study on the breakdown of the Mott insulator has not been done systematically so far, we think that this may provide an interesting subject in the correlated electron systems in non-equilibrium conditions.

ACKNOWLEDGMENTS

Note: We have quite recently noticed that Lehrer and Nelson [36] addressed the similar problem of the Mott transition empolying the boson Hubbard model.

* Present address: Institut für Theoretische Physik, Universität zu Köln, Zülpicher Strasse 77, 50937 Köln, Germany. Email: fukui@thp.uni-koeln.de

[1] J. G. Bednorz and K. A. M"uller, Z. Phys. B**64**, 189 (1986).

[2] As a review, see e.g. E. Dagotto, Rev. Mod. Phys. **66**, 763 (1994).

[3] P. W. Anderson, Science **235**, 1196 (1987).

[4] J. Hubbard, Proc. R. Soc. London, Ser. A276, 238 (1963); Ser. A281, 401 (1964).

[5] M. C. Gutzwiller, Phys. Rev. Lett. **10**, 159 (1963); W. F. Brinkman and T. M. Rice, Phys. Rev. **B2**, 4302 (1970).

[6] For recent advances in the theoretical study on the Mott insulators, see for example, A. Georges, G. Kotliar, W. Krauth and M. J. Rozenberg, Rev. Mod. Phys. **68**, 13 (1996).

[7] C. Kittel, *Introduction to Solid State Physics* (John Wiley & Sons, Inc., New York, 1996), and references therein.

[8] Y. Tokura, private communication. For related papers which have studied the dielectric breakdown of the charge ordered state for Mn oxides, see, A. Asamitsu, Y. Tomioka, H. Kuwahara, and Y. Tokura, Nature **388**, 50 (1997); K. Miyano, T. Tanaka, Y. Tomita, and Y. Tokura, Phys. Rev. Lett. **78**, 4257 (1997).

[9] W. Kohn, Phys. Rev. **133**, 171 (1964).

[10] B. S. Shastry and B. Sutherland, Phys. Rev. Lett. **65**, 243 (1990).

[11] B. Sutherland and B. S. Shastry, Phys. Rev. Lett. **65**, 1833 (1990).

[12] V. E. Korepin and A. C. T. Wu, Int. J. Mod. Phys. **B5**, 497 (1991).

[13] N. Yu and M. Fowler, Phys. Rev. **B46**, 14583 (1992).

[14] N. Hatano and D. R. Nelson, Phys. Rev. Lett. **77**, 570 (1997); cond-mat/9705290.

[15] R. A. Janik, M. A. Nowak, G. Papp and I. Zahed, cond-mat/9705098.

[16] P. W. Brouwer, P. G. Silvestrov and C. W. J. Beenakker, cond-mat/9705186.

[17] K. B. Effetov, cond-mat/9706055.

[18] E. Brézin and A. Zee, cond-mat/9708029.

[19] C. Mudry, B. D. Simons and A. Altland, cond-mat/9712103.

[20] N. M. Shnerb and D. R. Nelson, cond-mat/9801111.

[21] C. P. Yang, Phys. Rev. Lett. **19**,586 (1967); B. Sutherland, C. N. Yang and C. P. Yang, Phys. Rev. Lett. **19**, 588 (1967).

[22] I. M. Nolden, J. Stat. Phys. **67**, 155 (1992).

[23] D. J. Bukman and J. D. Shore, J. Stat. Phys. **78**, 1277 (1995).

[24] L. H. Gwa and H. Spohn, Phys. Rev. **A46**, 844 (1993).

[25] F. C. Alcaraz, H. Droz, M. Henkel and V. Rittenberg, Ann. Phys. **230**, 250 (1994).

[26] J. Neergaard and M. den Nijs, Phys. Rev. Lett. **74**, 730 (1995).

[27] D. Kim, Phys. Rev. **E52**, 3512 (1995).

[28] G. Albertini, S. R. Dahmen and B. Wehefritz, J. Phys. **A29**, L369 (1996); Nucl. Phys. **B493**, 541 (1997).

[29] J. D. Noh and D. Kim, cond-mat/9511001.

[30] N. Byers and C. N. Yang, Phys. Rev. Lett. **7**, 46 (1961).

[31] H. J. de Vega, Nucl. Phys. **B240**, 495 (1984).

[32] C. M. Yung and M. T. Batcherlor, Nucl. Phys. **B446**,

461 (1995).

[33] C. N. Yang, Phys. Rev. Lett. **19**, 1312 (1967).

[34] E. H. Lieb and F. Y. Wu, Phys. Rev. Lett. **20**, 1445 (1968).

[35] V. E. Korepin, N. M. Bogoliubov and A. G. Izergin, *Quantum Inverse Scattering Method and Correlation Functions*, (Cambridge University Press, 1993).

[36] R. A. Lehrer and D. R. Nelson, cond-mat/9806016.